International Journal of Innovative
Computing, Information and Control
Volume **8**, Number **9**, September **2012**

ICIC International ©2012 ISSN 1349-4198
pp. 6473–6489

SLIDING-MODE LOOP VOLTAGE CONTROL USING ASTRA-MATLAB INTEGRATION IN TOKAMAK REACTORS

M. Goretti Sevillano, Izaskun Garrido and Aitor J. Garrido

Department of Automatic Control and System Engineering
EUITI of Bilbao
University of the Basque Country
Plaza de la Casilla 3, 48012, Bilbao, Spain
{ mariagoretti.sevillano; izaskun.garrido; aitor.garrido }@ehu.es

Received June 2011; revised December 2011

Abstract. *The development of nuclear fusion as an alternative to fossil fuels and nuclear fission has motivated a growing interest in seeking solutions to the control problems existing in the nuclear fusion reactors such as Tokamaks. This paper considers the design of robust control schemes based on a sliding mode control to deal with the reference tracking problem for the loop voltage of a Tokamak by means of a control-oriented ASTRA-Matlab integration. The proposed controller stabilizes the system in spite of model uncertainties and the stability analysis of the closed-loop system dynamics is guaranteed by the Lyapunov stability theorem. The simulation results show the high-performance dynamic characteristics of the proposed method. The comparison of the simulation results provided by the sliding mode technique with those obtained from a traditionally used PID-based controller verifies that the proposed control scheme not only provides better tracking performance, but also faster and smoother response for the nonlinear system subject to model uncertainties and disturbances.*
Keywords: Plasma physics, Tokamak control, Modelling and simulation, Nonlinear control systems, Sliding mode control

1. **Introduction.** The current worldwide growth in energy demand together with the CO_2 emissions increment and the resulting climate change has promoted the research and development of new clean energy sources alternatives to fossil fuels and the potentially dangerous and controversial nuclear fission [1,2]. In this regard, substantial efforts and resources have been devoted to the development of clean nuclear technology based on fusion processes. In particular, as a result of this concern several researches are currently being carried out in the field of Control Engineering applied to fusion processes and reactors [3-6].

Thus, although the controlled fusion is still a technological challenge, fusion reactors present significant advantages over other energy sources, such as the existence of fuel supply for several thousand years or no contribution to air pollution, greenhouse effect or acid rain [5,7,8]. Furthermore, contrary to fission, it does not produce long-lived radioactive isotopes and it is intrinsically safe, so there is no risk of a large scale nuclear accident [4,5].

Nuclear fusion processes are based on the interaction of two light nuclei, contained in an ionized gas called plasma, which fuse into a heavier and more stable nucleus producing a large amount of energy [4,7,9,10]. This plasma can be confined using electromagnetic forces generated by external magnetic fields, which is known as magnetic confinement.

Nowadays, the most promising fusion reactor based on magnetic confinement is the Tokamak, which is basically a toroidal device (see Figure 1) that confines the hot plasma using a helical magnetic field [3-5,10,11].

Most of the controllers currently working on Tokamaks have been designed by decoupling the controls as much as possible. They are usually based on proportional integral derivative (PID) schemes with a multiloop structure, which are partly designed on the basis of simple models of the system to be controlled and they are usually fine-tuned during Tokamak operation. This decoupling has often implied the drawback of ignoring the effect on a particular plasma parameter from coils other than the coil being used to control that parameter. Besides, they do not take into account the sensitivity of the system to parameter uncertainties and disturbances. Therefore, recent efforts try to design more complex and robust controllers focusing the attention on these disadvantages [3-5,10].

Among various control schemes, variable structure control (VSC) has been considered as an effective method to deal with the control problems of nonlinear systems [12-15]. Therefore, in order to overcome the weakness of PIDs that have been extensively studied in literature [3-5,10,16] in this paper an integral sliding mode controller (ISMC) which constitutes a particular kind of VSC controllers is presented. For its design a control-oriented ASTRA-Matlab integration developed in previous works [16] has been used. This ISMC, unlike traditional variable structure designs [13-15], has an integral sliding surface [12,17-20]. The closed loop stability of the proposed scheme is demonstrated using the Lyapunov stability theory [12,21].

Given that Tokamaks are nonlinear systems with unavoidable model uncertainties and disturbances, which can lead to a performance degradation of the controlled system, it is necessary to study robust control schemes. In this sense, the sliding-mode control (SMC) presents many good characteristics over other control schemes, such as good performance against unmodelled dynamics, insensitivity to parameter uncertainties and variations, external disturbance rejection and fast dynamic response [12,13,15,22]. The simulation results provided in this paper suggest that the benefits provided by the SMC have made it possible to overcome the uncertainties arising from the difficulty of obtaining accurate

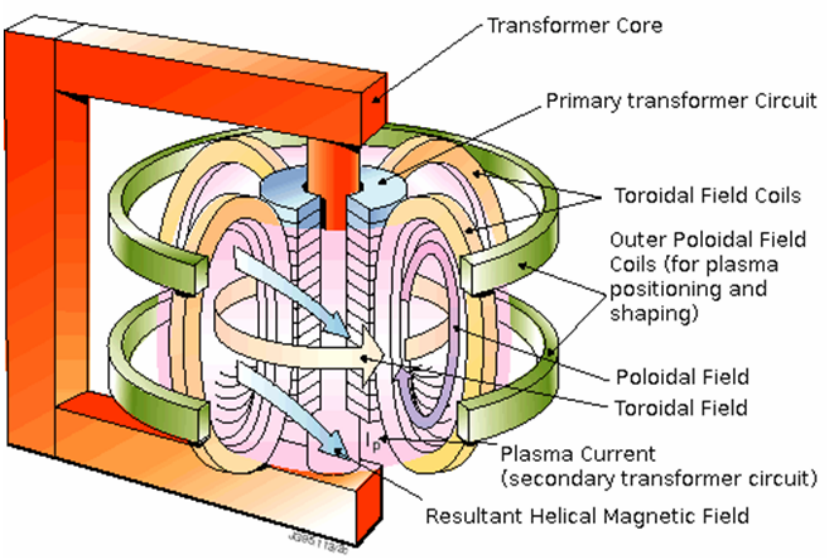

FIGURE 1. Scheme of a typical Tokamak

models of Tokamak plasmas or disturbances. This improved behaviour can also be deduced from the comparison of simulation results of the SMC with those obtained with a traditional PID that are given at the end of this manuscript.

The rest of the paper is organized as follows. In Section 2, the ASTRA Code used for modelling the Tokamak performance is presented. In Section 3, the control-oriented ASTRA-Matlab integration used for the design and study of the sliding-mode controller is described [16]. In Section 4, the mathematical model of the Tokamak used to design the controller is presented. Next, in Section 5 the proposed sliding-mode controller developed for the loop voltage is explained, where the simulation results are presented and compared with those obtained from a traditionally used Proportional Integral Derivative (PID) control scheme [4,5,16]. Finally, in Section 6, some concluding remarks end the article.

2. **ASTRA Code.**

2.1. **General description of the ASTRA code.** The ASTRA (Automatic System for Transport Analysis) is a widely used tool for generating computer code to simulate the transport in magnetically confined plasmas [9,23]. ASTRA solves coupled time-dependent 1-D transport equations for particles, heat and current and 2-D MHD (Magnetohydrodynamic) equilibrium self consistently with realistic Tokamak geometry.

The flexibility provided by ASTRA allows the user to customize the code and achieves higher efficiency. This flexibility relies on the wide choice of standard relationships, functions and subroutines that represent different transport coefficients, equilibrium solvers, auxiliary heating methods (e.g., NBI) and other physical processes and data processing in the Tokamak plasma. Another interesting feature of ASTRA is that it generates interactive codes which mean that the user, in addition to observing the time evolution of plasma parameters, can also interrupt the program execution or change the data layout in order to influence the course of modeling [23]. Therefore, the ASTRA code is considered a transport code with a flexible programming system able to create numerical codes for predictive or interpretative transport modeling, for stability analysis, and processing experimental data.

2.2. **ASTRA background equations and formulae.** In the ASTRA code, the magnetic system is considered to be toroidally symmetric and two coordinate systems are used: a cylindrical coordinate system (r, φ, z) with the polar axis coinciding with the major axis of the torus and another coordinate system (a, θ, ζ) associated with the magnetic geometry of the Tokamak where a denotes the radial variable which is an arbitrary label of a magnetic flux surface (see Figure 2), θ is the poloidal angle and the toroidal angle is chosen $\zeta = -\varphi$ [23]. The definition of the local flux g given by (1) and the condition for the function of magnetic surface $F(a)$ is expressed by means of the diffusion Equation (2), which requires the introduction of two functions of a single argument a defined by (3) and (4).

$$g(a,\theta) = F(a)\,\tilde{v}(a,\theta) - \tilde{D}(a,\theta)\,\nabla F(a) \tag{1}$$

$$\frac{\partial F}{\partial t} = \frac{\partial}{\partial V}\left(\left\langle (\nabla V)^2 \tilde{D}\right\rangle \frac{\partial F}{\partial V} - F\left\langle \nabla V \cdot \tilde{v}\right\rangle\right) + S(a) \tag{2}$$

$$D(a) = \left\langle (\nabla a)^2 \tilde{D}\right\rangle \Big/ \left\langle (\nabla a)^2\right\rangle \tag{3}$$

$$v(a) = \langle \nabla a \cdot \tilde{v}\rangle / \langle |\nabla a|\rangle \tag{4}$$

Considering those definitions independent of the choice of the magnetic surface label a it is possible to rewrite (2) in the form used in ASTRA (5). Using those definitions the

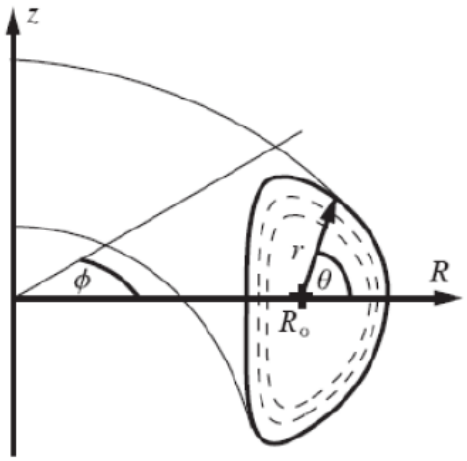

FIGURE 2. Axisymmetric configuration of the plasma (dashed lines represent the magnetic surfaces)

total flux and the average flux density on a magnetic surface can be expressed by (6) and (7) respectively.

$$\frac{\partial F}{\partial t} = \frac{\partial a}{\partial V}\frac{\partial}{\partial a}\left[\frac{\partial V}{\partial a}\left\langle(\nabla a)^2\right\rangle\left(D\frac{\partial F}{\partial a} - \frac{\langle|\nabla a|\rangle}{\left\langle(\nabla a)^2\right\rangle}vF\right)\right] + S\left(a\right) \tag{5}$$

$$\Gamma\left(a\right) = \frac{\partial V}{\partial a}\left(\langle|\nabla a|\rangle\, vF - \left\langle(\nabla a)^2\right\rangle D\frac{\partial F}{\partial a}\right) \tag{6}$$

$$\gamma\left(a\right) = vF - \frac{\left\langle(\nabla a)^2\right\rangle}{\langle|\nabla a|\rangle}D\frac{\partial F}{\partial a} \tag{7}$$

Thus, the magnetic field and the current density can be obtained by (8) and (9) respectively, where Ψ and I are defined by (10) and (11), being R_0 the distance from the axis of the torus to a fixed point in the plasma and B_0 the vacuum magnetic field at the point where $r = R_0$.

$$B = I\nabla\zeta + \frac{1}{2\pi}\left[\nabla\Psi \times \nabla\zeta\right] \tag{8}$$

$$j = -\frac{\nabla\zeta}{2\pi\mu_0}r^2 div\frac{\nabla\Psi}{r^2} + \frac{1}{\mu_0}\left[\nabla I \times \nabla\zeta\right] \tag{9}$$

$$\psi = -\Psi = \frac{1}{2\pi}\int\limits_V B\cdot\nabla\theta d^3x = \int\limits_{S_\theta} B\cdot dS_\theta \tag{10}$$

$$I = R_0B_0 - \frac{\mu_0}{2\pi}\int\limits_{S_\theta} j\cdot dS_\theta \tag{11}$$

The surface functions Ψ and I, depend on space coordinates through the variable a, so that they can be used as radial coordinate instead of a but they can also describe an evolving plasma through their dependence on time [23]. Once at this point, it is convenient to define another two surface functions: toroidal magnetic flux, Φ, and the effective minor

radius, ρ.

$$\Phi = \int\limits_{S_\zeta} B \cdot dS_\zeta = \frac{1}{2\pi} \int\limits_{V} \frac{I}{r^2} d^3x \tag{12}$$

$$\rho = \sqrt{(\Phi/(\pi B_0))} \tag{13}$$

The plasma equilibrium in a Tokamak is determined by the Grad-Shafranov Equation (14) [4,9,10], where $p = p(\rho, t)$ represents the plasma pressure with the contribution of all plasma species and I is the diamagnetic current (11).

$$\Delta^* \psi = r^2 div \frac{\nabla \psi}{r^2} = -4\pi^2 \left(\mu_0 r^2 \frac{\partial p}{\partial \psi} + I \frac{\partial I}{\partial \psi} \right) \tag{14}$$

The ASTRA code defines a special notation to simplify the equations which is explained in detail in [23]. It also uses the transport equations shown in Table 1 that may be expressed in terms of thermodynamic forces taken as derivatives with respect to ρ, which makes it possible to write the equilibrium Equation (14) in terms of the functions provided by transport equations as:

$$\Delta^* \psi = 2\pi \mu_0 R_0 \left[\frac{J}{\langle B^2/B_0^2 \rangle} \left(j_{||} + \frac{R_0}{B_0 \rho \mu} \frac{\partial p}{\partial \rho} \right) - \frac{r^2}{B_0 R_0 \rho \mu} \frac{\partial p}{\partial \rho} \right] \tag{15}$$

Table 1. Transport equations in ASTRA code

1. Equation for the electron density n_e, where Γ_e is the electron flux through a flux surface $\rho = const$ and S_e represents the source of electrons. $$\frac{1}{V'} \left(\frac{\partial}{\partial t} - \frac{\dot{B}_0}{2B_0} \frac{\partial}{\partial \rho} \rho \right) (V' n_e) + \frac{1}{V'} \frac{\partial}{\partial \rho} \Gamma_e = S_e$$
2. Equation for electron temperature T_e, where q_e is the electron heat flux through a flux surface $\rho = const$ and P_e represents the energy of the source of electrons. $$\frac{3}{2} (V')^{-5/3} \left(\frac{\partial}{\partial t} - \frac{\dot{B}_0}{2B_0} \frac{\partial}{\partial \rho} \rho \right) \left[(V')^{5/3} n_e T_e \right] + \frac{1}{V'} \frac{\partial}{\partial \rho} \left(q_e + \frac{5}{2} T_e \Gamma_e \right) = P_e$$
3. Equation for ion temperature T_i, where $n_i = n_e/Z_i$ and $\Gamma_i = \Gamma_e/Z_i$ and with q_i as the ion heat flux through a flux surface $\rho = const$ and P_i representing the energy of the source of ions. $$\frac{3}{2} (V')^{-5/3} \left(\frac{\partial}{\partial t} - \frac{\dot{B}_0}{2B_0} \frac{\partial}{\partial \rho} \rho \right) \left[(V')^{5/3} n_i T_i \right] + \frac{1}{V'} \frac{\partial}{\partial \rho} \left(q_i + \frac{5}{2} T_i \Gamma_i \right) = P_i$$
4. Equation for the poloidal flux ψ, where $\sigma_{||}$ represents the conductivity and by considering $\vec{j}_{BS}$ and $\vec{j}_{CD}$ as the bootstrap current density and the density of the current driven by external sources. $$\sigma_{||} \left(\frac{\partial \psi}{\partial t} - \frac{\rho \dot{B}_0}{2B_0} \frac{\partial \psi}{\partial \rho} \right) = \frac{J^2 R_0}{\mu_0 \rho} \frac{\partial}{\partial \rho} \left(\frac{G_2}{J} \frac{\partial \psi}{\partial \rho} \right) - \frac{V'}{2\pi\rho} (j_{BS} + j_{CD})$$

3. **ASTRA-Matlab Integration.** With the purpose of designing the SMC the control-oriented ASTRA-Matlab integration tool [16] described in this section has been used. In this tool, the standard ASTRA transport code for the simulation of Tokamaks is embedded in the Matlab-Simulink software (see Figure 3). On the one hand, this integration composes a very valuable tool for control design, since it offers to the researchers a useful tool for the development of different control schemes for various Tokamak models using the capabilities and benefits of the Simulink environment in an easy and intuitive way. On the other hand, there already exist different control codes that have been developed in Matlab, with accurate Tokamak description but lacking the capabilities of a transport code provided by ASTRA, which could benefit from this tool by developing coupled model control systems. Moreover, the incorporation of ASTRA transport code in Matlab allows inexpensive upgrades such as the implementation of high performance compilation if needed [16].

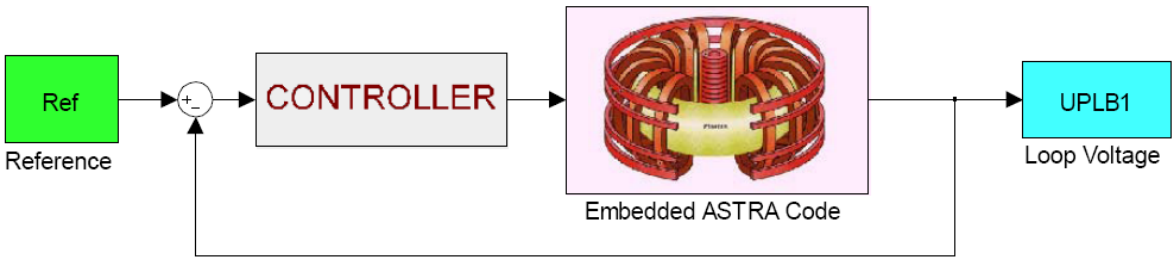

FIGURE 3. Simulink closed loop system diagram with embedded ASTRA code

The first step towards embedding ASTRA code into Matlab was the need to automate not only ASTRA execution through the process of saving-loading parameters but also to make the necessary modifications to maintain all the ASTRA capabilities. Therefore, two interface modules had to be programmed: the ASTRA-Matlab conversion and its corresponding inverse transformation. Besides, it was also necessary to create a C-module linked to the ASTRA code to automate the communication between both environments without the intervention of the user; the scheme of this software development can be observed in Figure 4.

Therefore, it is possible to consider that the integration can be divided into three main modules. The first one takes care of ASTRA Init and Interrupt routines by incorporating source code that implements specific functions to automate ASTRA execution. The second module modifies the initial and final values of each iteration. The third intermediate module transfers the output variables from the scope of ASTRA to the Simulink environment making the appropriate data conversion between both environments [16].

Using the features of Simulink tool interface the ASTRA can be embedded as a block in which all functions related to the ASTRA operation and its interconnection and communication with Matlab are collected. This block may be easily combined with other subroutines and control schemes without the need of further modifications.

The relevance of this integration relies in that there already exist several Matlab codes in the market lacking current profiles but integrating diverse Tokamak models. Therefore, the benefits of this integration are twofold: on the one hand, the control for the currents can be tested in Matlab via Simulink, and on the other hand, an inner second control loop may be implemented coupling ASTRA with another Tokamak model in order to extend the study and to control other variables as, for example, the vertical displacement of the plasma [24].

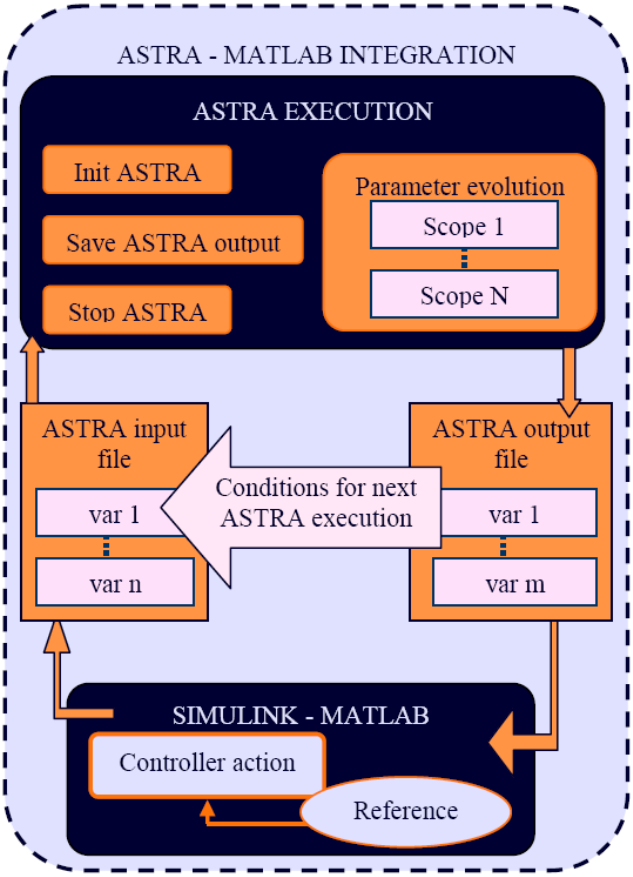

FIGURE 4. Software flow diagram of ASTRA automation

4. Mathematical Model of the System.

4.1. **Loop voltage.** In general, the loop voltage is defined as the voltage created in a circular loop concentric with the plasma column as a result of the variation of the poloidal magnetic flux linked through it (Figure 5, [24]). By extension of this concept, it can be defined in an arbitrary flux surface as minus the time derivative of the poloidal magnetic flux relative to that surface [24]. By inspection of Figure 5, it can be concluded that any change in the magnetic flux, ϕ, through the loop will generate a voltage, V, according to Lenz's law, $V = -d\phi/dt$. Flux changes can be produced by a variation in the plasma current or primary transformer flux. Since plasma and transformer circuits are inductively coupled, the loop voltage measurement contains mixed information regarding non-inductive current drive, plasma resistance and plasma inductance changes. The equivalent circuit of the Tokamak shows the relationship between the Tokamak equivalent parameters and loop voltage [11,23,25].

4.2. **Tokamak equivalent circuit and loop voltage state space model.** In order to adjust the controller parameters used in the simulations performed with the aforementioned ASTRA-Matlab integration, the state space model for the loop voltage described below has been used. In this model, the Tokamak is described as a distributed-parameter electric network [11,25,26]. Thus, the energy storage in the poloidal magnetic field is accounted for by a series inductance, L. The ohmic power loss in the plasma is represented by a series resistance, R. The total plasma current is denoted by I, and the non-inductive current drive can be described by a parallel current source, $\hat{I}$, or a series voltage supply,

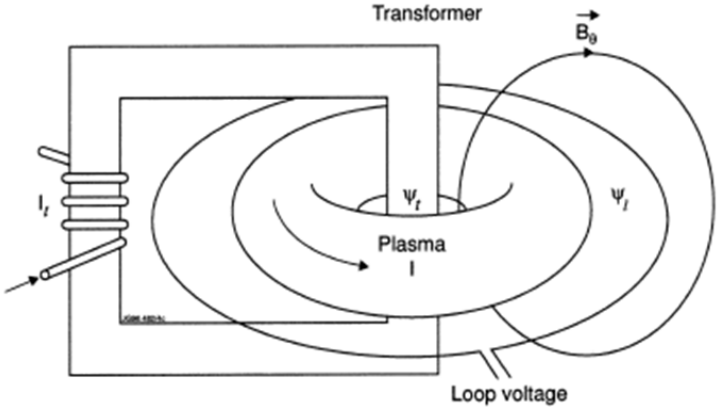

FIGURE 5. Simplified scheme of a Tokamak and the loop voltage measurements

$\hat{V} = R\hat{I}$. In this equivalent circuit the coupling between the plasma and the loop voltage is represented by a mutual inductance, M. It is assumed that the loop voltage, V, is measured along a poloidal flux surface, and its relationship with the distributed parameters can be given by:

$$V = RI - \hat{V} + \frac{d}{dt}\left(\left(L - M\right)I\right) \tag{16}$$

Moreover, applying the Poynting's theorem analysis to the poloidal magnetic field B_θ the energy balance equation can be expressed as

$$\frac{1}{2\mu_0}\frac{d}{dt}\int_\Omega B_\theta^2 dV + \int_\Omega \eta j_\phi^2 dV - \int_\Omega \eta j_\phi \hat{j}_\phi dV = VI \tag{17}$$

where μ_0 is the vacuum magnetic permeability, j_ϕ and $\hat{j}_\phi$ are the total and non-inductive plasma current profiles in the toroidal direction and η is the plasma resistivity profile.

The combination of (16) and (17) leads to (18) where the integration volume Ω is limited by the flux surface that intersects with the voltage loop. The volume Ω can be split into two regions Ω_i and Ω_e, which are internal and external to the plasma respectively. The internal region Ω_i is limited by the last closed flux surface (LCFS), while the external region Ω_e is limited externally by the flux surface that intersects the measuring loop and internally by the LCFS [11,25,26].

$$I\frac{d}{dt}\left(\left(L - M\right)I\right) = \frac{1}{2\mu_0}\frac{d}{dt}\int_\Omega B_\theta^2 dV \tag{18}$$

If Equation (18) is integrated in the interval $(0, t)$ the inductive elements $L - M$ can be written explicitly using (19) as a function of the internal and external inductances so that (16) may now be expressed as (20) [26]

$$L - M = \mu_0 \frac{r_0}{2}\left(l_i + l_e\right) \tag{19}$$

$$V = RI - \hat{V} + \mu_0 \frac{r_0}{2} I \frac{d}{dt}\left(l_i + l_e\right) + \mu_0 r_0 \left(l_i + l_e\right)\frac{dI}{dt} \tag{20}$$

When the loop voltage is calculated at the LCFS, $l_e = 0$, it is possible to rewrite (20) as it is shown in (21). Alternatively, if the effect of the non-inductive current is introduced as an ideal current source, $\hat{I}$, instead of the voltage, it is not subject to resistive losses

and the circuit equation can be expressed as (22) [26].

$$V_b = RI - \hat{V} + \mu_0 \frac{r_0}{2} I \frac{dl_i}{dt} + \mu_0 r_0 l_i \frac{dI}{dt} \tag{21}$$

$$V_b = R\left(I - \hat{I}\right) + \mu_0 \frac{r_0}{2} I \frac{dl_i}{dt} + \mu_0 r_0 l_i \frac{dI}{dt} \tag{22}$$

$$y = c_1 x_1 x_3 + c_2 \dot{x}_2 \tag{23}$$

Therefore, the loop voltage measurement given by (22) for constant plasma current can be written as the non-linear output Equation (23) for the state space model where $c_1 x_1 x_3 = R(I - \hat{I})$ and $c_2 \dot{x}_2 = \mu_0 \frac{r_0}{2} I \frac{dl_i}{dt}$.

Using this equivalent circuit representation it is possible to obtain a loop voltage state space model as a system of first-order differential equations where state space variables $X = (x_1, x_2, x_3)^T$ are chosen to correspond with physical meaningful quantities such as plasma resistance (whose dynamics can be approximated by the electronical temperature of the plasma T_e), internal inductance and ohmic current as it is shown in (24). The detailed description of the steps necessary to achieve the state space model can be found in [25,26].

$$X = \begin{pmatrix} x_1 \\ x_2 \\ x_3 \end{pmatrix} = \begin{pmatrix} \left\langle T_e^{-3/2} \right\rangle \\ l_i \\ I - \hat{I} \end{pmatrix} \tag{24}$$

Based on this state vector, the state space model can be approximated by a first order system as given in (25), whose parameters k_i and τ_i represent respectively the input gain, which can be estimated from the change in the states x_i once the stationary conditions are reached, and the time constant of the system, which for $i = 1$ is related to transport and current diffusion mechanisms in the plasma, for $i = 2$ is considered basically the skin time of the discharge and for $i = 3$ describes the dynamics of the ohmic part of the plasma current when a non inductive current is created in the plasma [26,27].

$$\dot{x}_i = -\frac{1}{\tau_i}\left(x_i - x_i|_{t=0}\right) + \frac{k_i}{\tau_i} u \tag{25}$$

5. **Sliding-Mode Controller for the Loop Voltage.**

5.1. **Introduction to sliding-mode controller (SMC).** Sliding-Mode Control is a technique derived from Variable Structure Control (VSC) which was originally studied by Utkin [15,27-29]. VSC consists of a set of continuous subsystems with a proper switching logic and, as a result, control actions are discontinuous functions of system states, disturbances (if they are accessible for measurement), and reference inputs [20,22,28]. Thus, the SMC is a nonlinear control strategy which is well-known for its robustness that has been developed and applied to closed-loop control systems for the past fifty years [18]. Also, the SMC makes it possible to replace generic nth order problems for equivalent simplified first order problems [30].

Because of the ability of this type of controllers to deal with non-linearities, time-dependency, as well as uncertainties and disturbances in a direct manner, these controllers can be applied to many different systems [12,18,20,28,31]. The control law defined in SMC is composed of two parts: on the one hand, the sliding-mode control law, which is responsible for maintaining the controlled system dynamics on a sliding surface and represents the desired closed loop behavior; on the other hand, the reaching mode control law which is designed in order to reach the desired surface [16].

The proposed sliding control scheme (see Figure 6) has been designed with the purpose of compensating the uncertainties of the system. In the sliding control theory, the switching gain must be chosen so that the sliding condition is verified [30]. In order to verify this condition, an appropriate choice of the sliding gain should be made to compensate these uncertainties. Although an upper bound of the parameter variations, unmodelled dynamics, noise magnitudes, etc. should be known to select the sliding gain, in practical applications those bounds are frequently unknown or very difficult to calculate. A solution to this problem is to choose a sufficiently high value for the sliding gain, assuring a control signal capable to overcome these drawbacks and achieve the control objective.

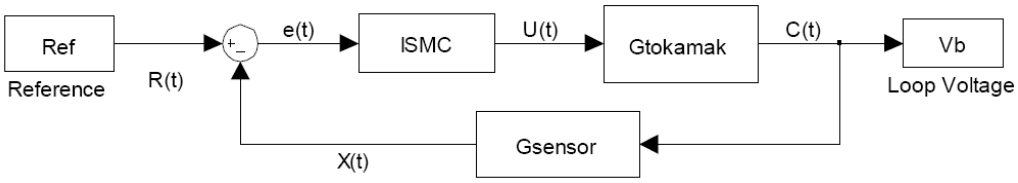

FIGURE 6. Scheme for sliding-mode controller (SMC)

5.2. **Design of the SMC for the loop voltage.** As it has been stated in the previous section the system dynamics can be expressed by (24) which may be rewritten as follows:

$$\dot{x}_i = -ax_i + b + cu \tag{26}$$

where $a = \frac{1}{\tau_i}$, $b = \frac{1}{\tau_i}\, x_i|_{t=0}$ and $c = \frac{K_i}{\tau_i}$.

Now, let us consider the previous dynamical Equation (26) with uncertainties as follows:

$$\dot{x}_i = -\left(a + \Delta a\right) x_i + \left(b + \Delta b\right) + \left(c + \Delta c\right) u \tag{27}$$

where the terms Δa, Δb and Δc represent the uncertainties of a, b and c respectively. It is assumed that these uncertainties are unknown but bounded.

And let us define the error as follows:

$$e(t) = \hat{x}\left(t\right) - x^*\left(t\right) = x\left(t\right) - x^*\left(t\right) - \tilde{x}\left(t\right) \tag{28}$$

where $\tilde{x}\left(t\right) = x\left(t\right) - \hat{x}\left(t\right)$ is the estimation error and $x^*\left(t\right)$ refers to the loop voltage command. Taking the derivative of (28) with respect to time yields

$$\dot{e}(t) = \dot{x}\left(t\right) - \dot{x}^*\left(t\right) - \dot{\tilde{x}}\left(t\right) = -ae\left(t\right) + g\left(t\right) + d\left(t\right) \tag{29}$$

where the following terms have been collected in the signal $g\left(t\right)$

$$g\left(t\right) = b + cu\left(t\right) - ax\left(t\right) - \dot{x}^*\left(t\right) \tag{30}$$

and the uncertainty terms have been collected in the signal $d\left(t\right)$

$$d\left(t\right) = -\Delta a x\left(t\right) + \Delta b + \Delta c u\left(t\right) - \dot{\tilde{x}}\left(t\right) \tag{31}$$

At this point, it should be noted that the term $d\left(t\right)$ is bounded because the terms Δa, Δb and Δc are bounded and the term $\dot{\tilde{x}}\left(t\right) = \dot{x}\left(t\right) - \dot{\hat{x}}\left(t\right)$ is also bounded, since both $\dot{x}\left(t\right)$ and $\dot{\hat{x}}\left(t\right)$ are bounded.

The first step in the design of the SMC is to define a sliding surface along which the process output can slide to find its desired final value. In general, the sliding surface should be designed to match the desired system dynamics because it represents the system behavior during the transient period [15]. This surface divides the phase plane into regions where the switching function $S\left(t\right)$ takes different sign. There are many options to select

this sliding variable $S(t)$; in this case a sliding variable with an integral component defined by (32) has been chosen [12,17,19] where k is a constant gain.

$$S(t) = e(t) - \int_0^t (k-a)\, e(\tau)\, d\tau \tag{32}$$

In order to achieve the reference tracking some assumptions have to be considered.

(**As. 1**) The gain k must be chosen so that the term $(k-a)$ is strictly negative, what is satisfied if $k < 0$ [19].

Now, it is possible to design the SMC as shown in (33), where k is the gain previously defined, β is the switching gain, S is the sliding surface defined by (32) and sgn () is the sign function applied for achieving better tracking performance [12]:

$$g(t) = ke(t) - \beta \mathrm{sgn}(S) \tag{33}$$

(**As. 2**) The gain β must be chosen so that $\beta > |d(t)|$ at any time. It should be noted that this assumption implies that an upper bound for the uncertainties is known.

After the sliding surface has been selected, the control law must be designed to satisfy the condition $S(t) = 0$ [17,19,27]. In addition, the problem of tracking a reference value can be reduced to that of keeping $S(t)$ at zero and, once $S(t) = 0$ is reached, to satisfy the sliding condition defined by (34) in order to guarantee the value of $S(t)$ at zero.

$$\frac{dS(t)}{dt} = 0 \quad \text{(Sliding condition)} \tag{34}$$

This condition can be derived from the Lyapunov stability theory as it may be observed in the following proof where (32), (33), (36) and the assumption (**As. 2**) are used.

Let the Lyapunov function be defined as [12,19,21,27]

$$V(t) = \frac{1}{2} S(t)\, S(t) \tag{35}$$

The derivative of this candidate is calculated as follows

$$\begin{aligned} \dot{V}(t) &= S(t)\, \dot{S}(t) \\ &= S \cdot [\dot{e} - (k-a)\, e] \\ &= S \cdot [(-ae + g + d) - (ke - ae)] \\ &= S \cdot [g + d - ke] \\ &= S \cdot [ke - \beta \mathrm{sgn}(S) + d - ke] \\ &= S \cdot [d - \beta \mathrm{sgn}(S)] \\ &\leq -(\beta - |d|)\, |S| \\ &\leq 0 \end{aligned} \tag{36}$$

Using the Lyapunov's direct method, since $V(t)$ is clearly positive definite, $\dot{V}(t)$ is negative semidefinite and $V(t)$ tends to infinity as $S(t)$ tends to infinity, it implies that the equilibrium at the origin $S(t) = 0$ is globally asymptotically stable. Therefore, $S(t)$ tends to zero as time tends to infinity. Moreover, all trajectories starting off the sliding surface $S(t) = 0$ must reach it in finite time and then they will remain on this surface. This behavior of the system on the sliding surface is usually called sliding-mode [19].

When the sliding-mode occurs on the sliding surface (32), $S(t) = \dot{S}(t) = 0$, the dynamical behavior of the tracking problem defined by (29) is equivalently governed by:

$$\dot{e}(t) = (k-a)\, e(t) \tag{37}$$

It should be noted that a typical motion under SMC consists of a reaching phase during which trajectories starting off the sliding surface $S = 0$ move towards it and reach it in a finite time, followed by sliding phase during which the motion will be confined to this surface and the system error will be represented by the reduced order model (37), where the error tends to zero. Then according to assumption (**As. 1**), the error $e(t)$ converges to zero exponentially.

The second term of the right hand side of (33) represents the discontinuous part of the control law, which is nonlinear and represents the switching element of the control law across the sliding surface. Although, hypothetically, this control law should allow changes between structures infinitely fast, in practice, due to finite time delays in control computations or limitations of the physical actuators, it is not possible to reach such a high speed switching control; therefore chattering around the sliding surface appears [15,22]. The sliding surface reaching time depends on the control gain, but it must be taken into account that if the controller is too aggressive it can contribute to the chattering [32].

5.3. **Simulation results.** In this section some simulation results are shown in order to illustrate the effectiveness of the proposed sliding-mode controller for the loop voltage in a reference tracking problem through simulation examples using the ASTRA-Matlab integration tool for which no other conditions or restrictions but those imposed by the model assumed in the ASTRA code [16].

The block diagram of the proposed control scheme has been presented in Figure 3, where the block "Controller" corresponds to the sliding-mode controller detailed in the previous section and described by (33), while the block "Embedded ASTRA Code" represents the control-oriented ASTRA-Matlab integration presented in the third section of this paper.

In the examples, the loop voltage is controlled by manipulating the plasma current, where the values for the sliding control law parameters have been chosen according to the assumptions and considerations exposed in Section 5.2 for two different switching gains. Simulation results given in Figure 7 represent the time evolution for the desired loop voltage that are obtained from the simulation of the system using the SMC1 (see Table 2). It can be appreciated that after a transitory time the loop voltage tracks the desired reference in spite of a 20% of system uncertainties considered in the ohmic current and coil parameters.

TABLE 2. Sliding-mode controllers parameters

SMC1	$k = -30$	$\beta = 20$
SMC2	$k = -30$	$\beta = 40$

However, in Figure 7 it may also be appreciated the presence of the so-called chattering phenomenon in the controlled variable with high frequency changes inherent to the use of a sliding-mode controller. As it has been indicated, the presence of this chattering phenomenon is due to the discontinuities of the sliding control law across the sliding surface which forces the switching function $S(t)$ given by (32) to take different sign.

Finally, the optimization of the controller parameters makes it possible to improve the simulation results, as it may be inferred comparing the simulation results obtained for SMC1 with those obtained for SMC2. In this sense, Figure 8 shows the loop voltage obtained from the simulation using SMC2 and its corresponding reference. Comparing the loop voltage response for SMC1 depicted in Figure 7 and the one for the SMC2 shown in Figure 8, it is shown that the system response is faster with a lower settling time but that the chattering observed in this last simulation is bigger than that in the first one. This may also be observed from the tracking error of the loop voltage shown in Figure 9

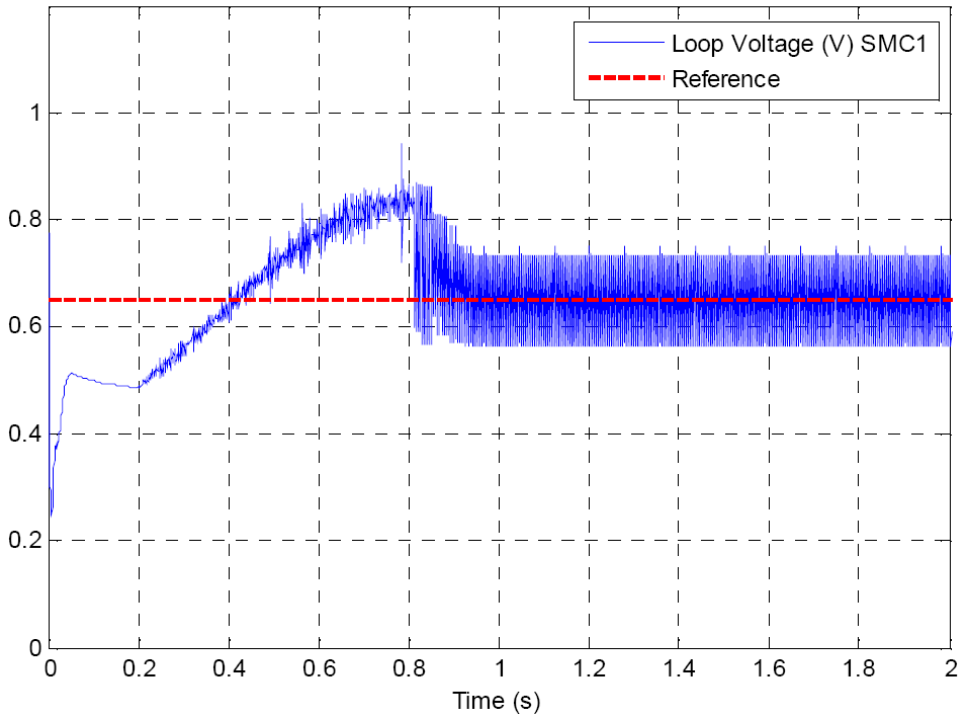

FIGURE 7. Controlled variable (loop voltage) for SMC1

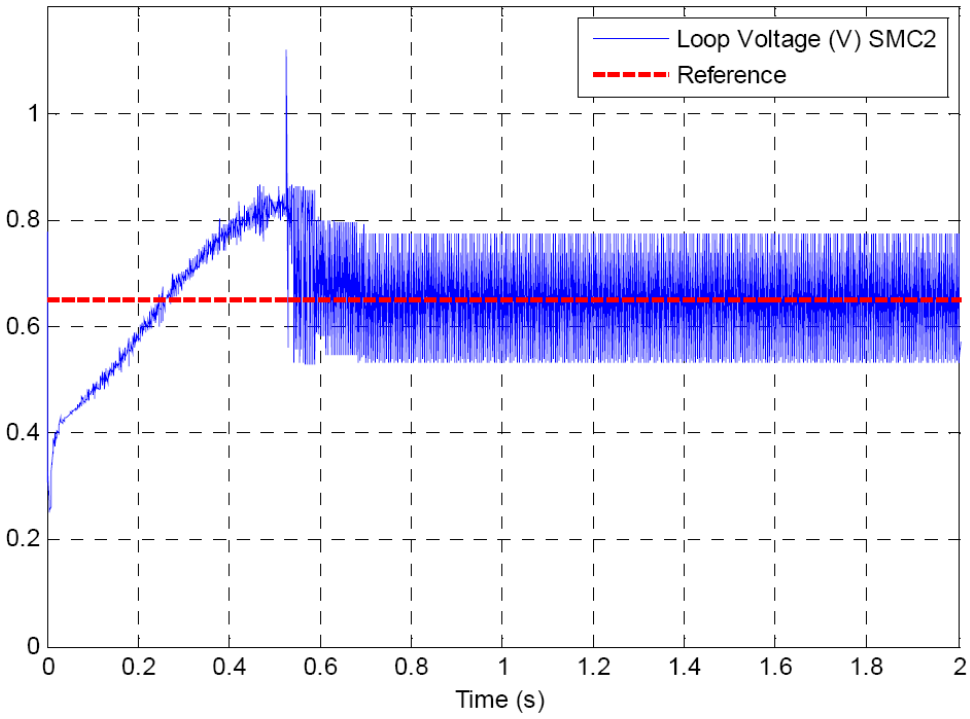

FIGURE 8. Controlled variable (loop voltage) for SMC2

where the amplitude of the chattering present in the error signal is higher for SMC2 than that for SMC1, as it could be expected since SMC2 uses a higher value of the switching gain β.

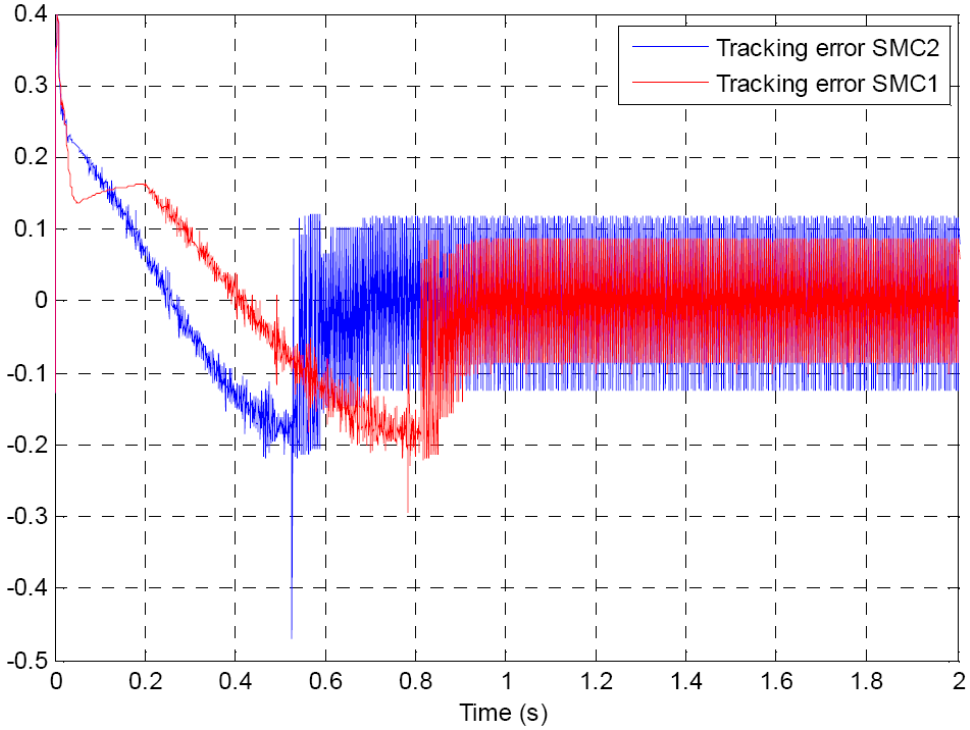

FIGURE 9. Tracking error for SMC

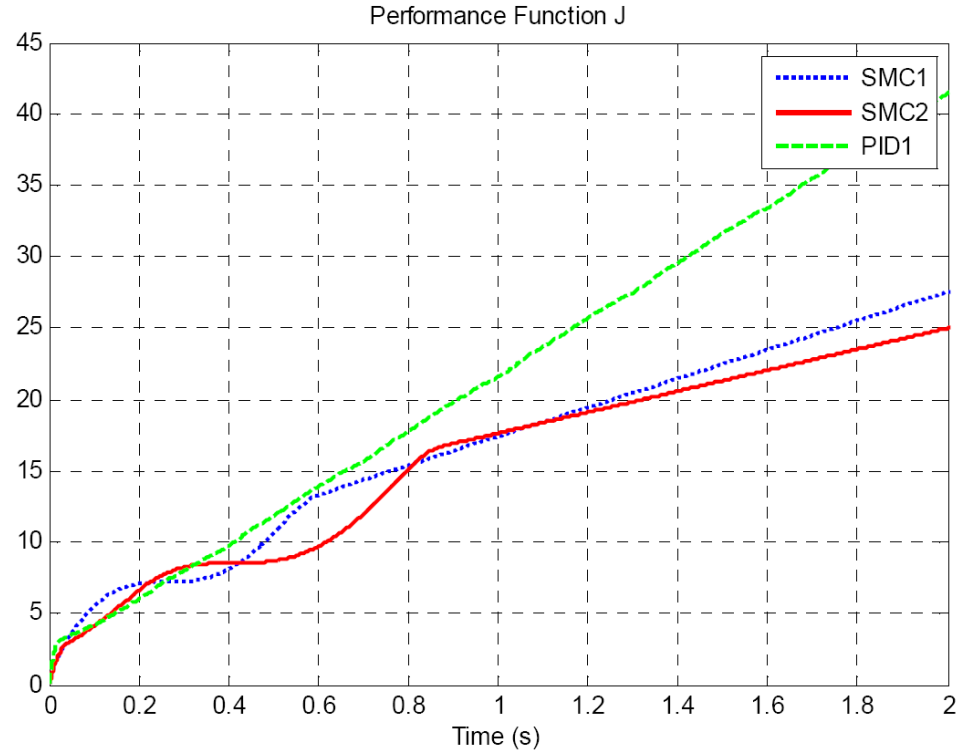

FIGURE 10. Performance functions for SMC1, SMC2, and for the traditional PID controller

5.4. **Comparative of simulation results.** In this section, a comparison of the simulation results obtained using the proposed SMC with those obtained using a traditional PID-based controller is given so as to exemplify the better performance of this robust scheme [4,5,16]. For this purpose, a performance evolution function J is used. This performance function is defined by (38) in terms of the tracking error, where $e(\tau)$ represents the error between the desired reference value for the loop voltage and the value obtained from the system output.

$$J(t) = \int e^2(\tau)\, d\tau \tag{38}$$

It can be observed in Figure 10 that the performance function for the SMC2 presents a value lower than the one for SMC1 as it may be expected due to the mentioned reduction of the chattering in the output of the system and the improvement in system response speed. It can also be observed that the value of the performance evolution function for the case of the PID-based controller is higher than the one for the sliding mode controllers. It must be taken into account that, although the PID-based controlled has been adequately tuned with a robust quarter decay ratio step response for the Tokamak system plant, it is not able to deal with the 20% of system uncertainties considered. For this reason, although in all cases the accumulated error measured with the cost function J defined above presents an increasing behavior, it can be noticed that the growth rate is much higher for the PID-based controller than that for SMC controllers since the error added in SMC controllers is stabilized in the steady-state. At this point, it may be noted that although the SMC controllers adequately match the desired reference input, the performance evolution functions exhibit this increasing behavior due to the presence of undesired chattering phenomenon in the error signals.

6. **Conclusions.** The aim of this paper has been the design of a sliding-mode controller to deal with a reference tracking problem for the loop voltage of a Tokamak using the control-oriented ASTRA-Matlab integration. The steps followed to implement the desired controller show the feasibility of the integration used, as a valuable tool for the development of controllers for Tokamak reactors in an easy and unified way. In this sense, the ASTRA-Matlab integration allows the use of the Simulink toolbox for the control design, providing users with the ability to try and test different controllers in a more convenient way with the final aim of facilitating the development and application of advanced control schemes to the widely extended and standardized ASTRA code for Tokamak reactors.

The simulation results obtained for the sliding-mode controller with an integral component presented in this paper have shown a better performance than a traditional PID-based scheme despite system uncertainties. Considering the difficulty to achieve accurate models for Tokamak plasmas the feasibility and effectiveness of robust controllers with important features such as disturbance rejection, uncertainty insensitivity and fast response it is very desirable for practical implementation.

Acknowledgment. The authors are very grateful to the University of the Basque Country (UPV/EHU) through Research Project GIU11/02. They are also grateful to the Science and Innovation Council MICINN for its support through research project ENE2010-18345. They are also grateful for its support to the EU FP7 EFDA under the task WP09-DIA-02-01 WP III-2-c. The authors also gratefully acknowledge the helpful comments and suggestions of the reviewers, which have improved the presentation.

REFERENCES

[1] Shell International, Global Business Environment, *Energy Needs, Choices and Possibilities: Scenarios to 2050*, 2001.

[2] P. B. Weisz, Basic choices and constraints on long-term energy supplies, *Physics Today*, vol.57, pp.47-52, 2004.

[3] M. Ariola and A. Pironti, *Magnetic Control of Tokamak Plasmas*, Springer, 2008.

[4] A. Pironti, M. Walker, M. Ariola et al., Special section on control of fusion – Various authors, *IEEE Control Systems Magazine*, vol.25, no.5, pp.24-92, 2005.

[5] A. Pironti, M. Walker, J. B. Lister et al., Special section on control of fusion: Part II – Various authors, *IEEE Control Systems Magazine*, vol.26, no.2, pp.30-91, 2006.

[6] M. G. Sevillano, I. Garrido, A. J. Garrido et al., Observer-based real-time control for the poloidal beta of the plasma using diamagnetic measurements in Tokamak fusion reactors, *The 50th IEEE Conference on Decision and Control and European Control Conference*, 2011.

[7] *ITER Web Site*, http://www.iter.org/, 2011.

[8] M. Amundarain, M. Alberdi, A. J. Garrido and I. Garrido, Modeling and simulation of wave energy generation plants: Output power control, *IEEE Transactions on Industrial Electronics*, vol.58, no.1, pp.105-117, 2011.

[9] A. Garrido, I. Garrido, O. Barambones and P. Alkorta, A survey on control-oriented plasma physics in tokamak reactors, *Proc. of the 5th International Conference on Heat Transfer, Thermal Engineering and Environment*, pp.284-289, 2007.

[10] J. Wesson, *Tokamaks*, 3rd Edition, Clarendon Press, Oxford, UK, 2004.

[11] A. Garrido, I. Garrido, O. Barambones, P. Alkorta and F. J. Maseda, Simple linear models for plasma control in Tokamak reactors, *Proc. of the IEEE International Conference on Control, Automation and Systems*, pp.2429-2432, 2008.

[12] C.-C. Peng, Y. Li and C.-L. Chen, A robust integral type backstepping controller design for control of uncertain nonlinear systems subject to disturbance, *International Journal of Innovative Computing, Information and Control*, vol.7, no.5(A), pp.2543-2560, 2011.

[13] Q. P. Ha, D. C. Rye and H. F. Durrang-Whyte, Robust sliding mode control with application, *International Journal of Control*, vol.72, no.12, pp.1087-1096, 1999.

[14] F. Plestan, Y. Shtessel, V. Brégeault and A. Poznyak, New methodologies for adaptative sliding mode control, *International Journal of Control*, vol.83, no.9, pp.1907-1919, 2010.

[15] V. I. Utkin, Sliding mode control design principles and applications to electric drives, *IEEE Transactions on Industrial Electronics*, vol.40, no.1, pp.23-36, 1993.

[16] M. G. Sevillano, I. Garrido and A. J. Garrido, Control-oriented automatic system for transport analysis (ASTRA)-matlab integration for Tokamaks, *Energy*, vol.36, no.5, pp.2812-2819, 2011.

[17] O. Barambones, M. De La Sen and P. Alkorta, A robust control of double-feed induction generator for wind power generation, *The 35th Annual Conference of IEEE Industrial-Electronics-Society*, vol.1-6, pp.84-89, 2009.

[18] J. Lian, J. Zhao and G. M. Dimirovski, Model reference adaptive integral sliding mode control for switched delay systems, *International Journal of Innovative Computing, Information and Control*, vol.4, no.8, pp.2025-2032, 2008.

[19] O. Barambones, A. J. Garrido and F. J. Maseda, Integral sliding-mode controller for induction motor based on field-oriented control theory, *IET Control Theory and Applications*, vol.1, no.3, pp.786-794, 2007.

[20] C. Edwards and S. K. Spurgeon, *Sliding Mode Control*, Taylor & Francis, London, U.K., 1998.

[21] C. F. Alastruey and M. De La Sen, Stability of time-delay systems via Lyapunov functions, *Mathematical Problems in Engineering*, vol.8, no.3, pp.197-205, 2002.

[22] Y. Xia, H. Yang, M. Fu and P. Shi, Sliding mode control for linear systems with time-varying input and state delays, *Circuits, Systems, and Signal Processing*, vol.30, no.2, pp.629-641, 2011.

[23] G. V. Pereverzev and P. N. Yushmanov, *Automated System for Transport Analysis*, Max-Planck-Institut für Plasmaphysik, 2002.

[24] J. A. Romero, J. M. de la Cruz, T. Dobbing, J. Ellis, B. Fisher, Q. A. King, F. Söldner and N. Zornig, Real time current profile control at JET, *Fusion Engineering and Design*, vol.43, no.1, pp.37-58, 1998.

[25] J. A. Romero, *Análisis, modelado y utilización de diagnósticos magnéticos en el control del perfil de corriente en el tokamak JET*, Ph.D. Thesis, UNED, Madrid, Spain, 1997.

[26] S. Sharma, D. J. N. Limebeer, I. M. Jaimoukha and J. B. Lister, Modeling and control of TCV, *IEEE Transactions on Control Systems Technology*, vol.13, no.3, pp.356-369, 1995.

[27] O. Camacho, R. Rojas and W. García, Variable structure control applied to chemical processes with inverse response, *ISA Transactions*, vol.38, no.1, pp.55-72, 1999.
[28] J. J. E. Slotine and W. Li, *Applied Nonlinear Control*, Prentice Hall, NJ, USA, 1991.
[29] V. I. Utkin, *Sliding Modes in Control and Optimization*, Springer – Verlag, 1992.
[30] M. Pérez de la Parte, O. Camacho and E. F. Camacho, Development of a GPC-based sliding mode controller, *ISA Transactions*, vol.41, no.1, pp.19-30, 2002.
[31] J. Y. Hung, Variable structure control: A survey, *IEEE Transactions on Industrial Electronics*, vol.40, no.1, pp.2-22, 1993.
[32] O. Camacho, R. Rojas and W. García-Gabín, Some long time delay sliding mode control approaches, *ISA Transactions*, vol.46, no.1, pp.95-101, 2007.